Third AO4ELT Conference - Adaptive Optics for Extremely Large Telescopes
Florence, Italy. May 2013
ISBN: 978-88-908876-0-4
DOI: 10.12839/AO4ELT3.13505

DECONVOLUTION-BASED SUPER-RESOLUTION FOR POST-ADAPTIVE-OPTICS DATA

Marcel Carbillet[1a], Andrea La Camera[2b], Olivier Chesneau[3], Florentin Millour[3], Julien H. V. Girard[4], and Marco Prato[5]

[1] UMR 7293 Lagrange (Université de Nice Sophia-Antipolis/CNRS/Observatoire de la Côte d'Azur), Parc Valrose, 06100 Nice, France
[2] Dipartimento di Informatica, Bioingegneria, Robotica e Ingegneria dei Sistemi (Università di Genova), Via Dodecaneso 35, 16145 Genova, Italia
[3] UMR 7293 Lagrange (Université de Nice Sophia-Antipolis/CNRS/Observatoire de la Côte d'Azur), Boulevard de l'Observatoire, BP 4229, 06300 Nice, France
[4] European Southern Observatory, Casilla 19001, Vitacura, Santiago, Chile
[5] Dipartimento di Scienze Fisiche, Informatiche e Matematiche (Università di Modena e Reggio Emilia), Via Campi 213/b, 41125 Modena, Italia

Abstract. This article presents preliminary results on NACO/VLT images of close binary stars obtained by means of a Richardson-Lucy-based algorithm of super-resolution, where down to roughly a half-resolution element is attained, and with confirmation from VLTI observations in one of the cases treated. A new gradient method, the scaled gradient projection (SGP), permitting the acceleration of the used method, is also tested with the same scope.

1 Introduction

Super-resolution is a term which classically refers to methods aiming at going beyond the diffraction limit of an optical instrument such as a telescope. In our case, which is actually not relevant to a specific type of instrument but to the post-processing of the data obtained, we would rather use the term *computational super-resolution* (CSR). It is worthwhile to immediately note that CSR is not feasible in all situations/observational conditions, and, when it is possible, it is never unlimited [1].

The ideal angular resolution of a circular telescope is usually approximated by λ/D (where λ is the observing wavelength and D the diameter of the entrance pupil of the telescope, and forgetting for now about all the internal and atmospherically-induced aberrations which would dramatically enlarge it), which is roughly the full width at half-maximum (FWHM) of the Airy disc and (hence!) the empirical Dawes' limit, practically much rather used than the (somehow conservative) Rayleigh criterion, $1.22\,\lambda/D$.

CSR aims at breaking (when possible) this λ/D resolution limit by means in the present paper of deconvolution which, in addition to pretend to correct for the various residual aberrations due to the turbulent atmosphere, the adaptive optics (AO) system trying to correct from the effects of the latter, the telescope, and the imaging instrument, also pretends here to correct from the degradation due to diffraction.

[a] marcel.carbillet@unice.fr
[b] andrea.lacamera@unige.it

This basically translates into extrapolation of the Fourier spectrum of the image outside of the transmission band of the global imaging system (atmosphere⊕telescope⊕instrument), i.e. beyond the limiting angular frequency D/λ. See again Bertero & Boccacci [1] for a complete description of this out-of-band process.

In the case of post-AO astronomical imaging, it has been demonstrated (although by means of numerical simulations) that, in case of relatively high signal-to-noise ratio and relatively good AO correction, a gain of a factor 4 to 5 in resolution can be achieved [6]. A necessary condition anyway is also the fact that the object must be compact, with an angular size of the order of, or smaller than, λ/D.

Here, with real data and no particular careful pre-processing of it, and a very low angular sampling (e.g. large pixel size) with respect to the scopes of the method, we reach roughly half a resolution element, which can be considered as an encouraging starting point.

The paper is organised as follows. Next section, Sec. 2, presents the Richardson-Lucy (RL) method and its origins. Then, Sec. 3 exposes the CSR algorithm based on the RL method itself, and Sec. 4 proposes an alternative version of it, accelerated by means of the scaled gradient projection (SGP) method. Then, Sec. 5 shows and comments on the preliminary results obtained from VLT/NACO data of close binary stars in the wavebands K_s and L. Finally, Sec. 6 draws up a summary of the work performed up to now and gives our conclusions and perpectives for the next future.

2 Richardson-Lucy deconvolution method

Let us define $\mathbf{f}$ as the scientific target, $\mathbf{g}$ the acquired image to be deconvolved, $\mathbf{b}$ the sky background, and A the imaging matrix given by $A\mathbf{f} = \mathbf{K} * \mathbf{f}$, where $*$ is the convolution operator and K is the point-spread function (PSF), normalized to a unit volume. In the case of Poisson noise, the general approach to the deconvolution methods follows the minimization of the Kullback-Leibler (KL) divergence given by:

$$J_0(\mathbf{f};\mathbf{g}) = \sum_{\mathbf{m}\in S}\left\{\mathbf{g}(\mathbf{m})\ln\frac{\mathbf{g}(\mathbf{m})}{(A\mathbf{f})(\mathbf{m})+\mathbf{b}(\mathbf{m})} + (A\mathbf{f})(\mathbf{m}) + \mathbf{b}(\mathbf{m}) - \mathbf{g}(\mathbf{m})\right\} . \tag{1}$$

From well-known properties of this functional, it follows that J_0 is *non-negative*, *convex*, and *coercive*. So that absolute minimizers of this function exist: the so-called *maximum likelihood* solutions of the image reconstruction problem. The RL method [2,3] follows from the computation of the gradient of J_0 and the application of the Karush-Kuhn-Tucker conditions. It is described in Algorithm 1.

Algorithm 1 RL method

Choose the starting point $\mathbf{f}^{(0)} \geq 0$

For $k = 0, 1, 2, \ldots$ compute:

$$\mathbf{f}^{(k+1)} = \mathbf{f}^{(k)} A^T \frac{\mathbf{g}}{A\mathbf{f}^{(k)} + \mathbf{b}}$$

End

3 Richardson-Lucy-based super-resolution

The global method used in this paper is based on the well-known property of RL which allows CSR [4,5,1]. It consists in the following two steps, as described in Anconelli et al. [6]

- STEP 1 – Compute a large number of RL iterations, assuming a constant array as initial guess of the algorithm. We denote the result of this step by $\mathbf{f_1}$.
- STEP 2 – Define the (compact) support $\mathcal{S}$ of the object as the pixels where the flux of $\mathbf{f_1}$ is greater than a selected threshold, or alternatively an area of angular dimension of the order of the resolution element of the data, λ/D. Next, initialize the algorithm using the mask with pixels set to one inside and to zero outside the domain $\mathcal{S}$. Then, compute again a large number of RL iterations, obtaining the final reconstructed image $\mathbf{f_2}$.

The CSR method described above and used in the following is implemented within the last distributed versions of the `Software Package AIRY` [7,8], developed within the `CAOS` problem-solving environment (`PSE`) [9,10], and used in the following of the paper.

4 Scaled gradient projection acceleration

The RL algorithm can be seen as a particular case of a scaled gradient method. Indeed, since

$$\mathbf{f}^{(k+1)} = \mathbf{f}^{(k)} - \mathbf{f}^{(k)}\left(\mathbf{1} - A^T\frac{\mathbf{g}}{A\mathbf{f}^{(k)} + \mathbf{b}}\right) = \mathbf{f}^{(k)} - \mathbf{f}^{(k)}\nabla J_0(\mathbf{f}^{(k)}; \mathbf{g}) \,, \tag{2}$$

it follows that the RL iteration can be obtained from the general scaled gradient algorithm:

$$\mathbf{f}^{(k+1)} = \mathbf{f}^{(k)} - \lambda_k(P_+(\mathbf{f}^{(k)} - \alpha_k D_k \nabla J_0(\mathbf{f}^{(k)}; \mathbf{g})) - \mathbf{f}^{(k)}) \,, \tag{3}$$

by choosing the constant steplengths $\lambda_k = \alpha_k = 1$, the scaling matrix $D_k = \mathrm{diag}(\mathbf{f}^{(k)})$, and by remarking that for RL the projection P_+ on the non-negative pixels can be avoided since it is automatically satisfied by the iteration.

The choice of constant steplengths makes RL not very efficient and several acceleration schemes have been proposed in the literature to improve its convergence rate. The SGP method [11] is an optimization method for the minimization of the KL divergence that uses the scaling of the gradient suggested by RL, but exploits an adaptive strategy for the steplength parameters. For this reason, SGP can be considered as a more efficient version of RL.

The SGP scheme is described in Algorithm 2. For a general version of the algorithm and, in particular, for the computation of the steplength parameter α_k, we refer to Bonettini et al. [11] and Prato et al. [12]

Algorithm 2 SGP method

Choose the starting point $\mathbf{f}^{(0)} \geq 0$ and set the parameters $\beta, \theta \in (0,1)$, $0 < \alpha_{min} < \alpha_{max}$.

FOR $k = 0, 1, 2, \ldots$ DO THE FOLLOWING STEPS:

STEP 1. Choose the parameter $\alpha_k \in [\alpha_{min}, \alpha_{max}]$ and the scaling matrix D_k;

STEP 2. Projection:

$$\mathbf{y}^{(k)} = P_+(\mathbf{f}^{(k)} - \alpha_k D_k \nabla J_0(\mathbf{f}^{(k)}; \mathbf{g}));$$

STEP 3. Descent direction: $\mathbf{d}^{(k)} = \mathbf{y}^{(k)} - \mathbf{f}^{(k)}$;

STEP 4. Set $\lambda_k = 1$;

STEP 5. Backtracking loop:

IF $J_0(\mathbf{f}^{(k)} + \lambda_k \mathbf{d}^{(k)}; \mathbf{g}) \leq J_0(\mathbf{f}^{(k)}; \mathbf{g}) + \beta \lambda_k \nabla J_0(\mathbf{f}^{(k)}; \mathbf{g})^T \mathbf{d}^{(k)}$

THEN go to step 6;

ELSE set $\lambda_k = \theta \lambda_k$ and go to step 5.

ENDIF

STEP 6. Set $\mathbf{f}^{(k+1)} = \mathbf{f}^{(k)} + \lambda_k \mathbf{d}^{(k)}$.

END

The acceleration of the CSR can be obtained applying the same scheme described in previous section, replacing RL with SGP. The SGP method will be implemented in the next distributed version of the `Software Package AIRY`.

We apply in the following the two methods described to NACO/VLT data of very close binary stars, but in the case of SGP we push the algorithm to convergence, i.e. we compute the *objective function* $J_0(\mathbf{f}^{(k)}; \mathbf{g})$ at each iteration and we stop the iteration when this function is (almost) constant — i.e., according to a given tolerance ϵ, when

$$|J_0(\mathbf{f}^{(k)}; \mathbf{g}) - J_0(\mathbf{f}^{(k-1)}; \mathbf{g})| < \epsilon \cdot J_0(\mathbf{f}^{(k)}; \mathbf{g}) \, . \tag{4}$$

5 Preliminary results on NACO/VLT data

The data presented in this section were obtained by using the NACO adaptive optics camera (NAos adaptive optics system combined with the COnica camera, see Rousset et al. [13]) attached to the telescope UT 4 of the Very Large Telescope (VLT).

HD 87643

The data considered here are K_s-band data (2.18-μm) obtained with NACO/VLT and already analyzed by Millour et al. [14] together with VLTI observations of the same object: HD 87643. A first deconvolution of the NACO/VLT data has already also been presented in Le Bouquin et al. [15], but in both cases the (very close) binary star could not have been resolved. At the opposite, in Millour et al. [14], the observations of the same object using the interferometric instrument AMBER onboard the VLTI (the VLT long-baseline interferometer) clearly showed the binarity of the source.

The data analyzed here were taken with an atmospheric seeing of $\sim$0.″9, a total exposure time of $\sim$90 s, and by using camera mode S 13, with a pixel size of 13 mas and a 14″×14″ field of view. The Strehl ratio associated to these data is estimated to be 0.43±0.04, which is somehow limited with respect to the limitations expected for this method (see Sec. 1).

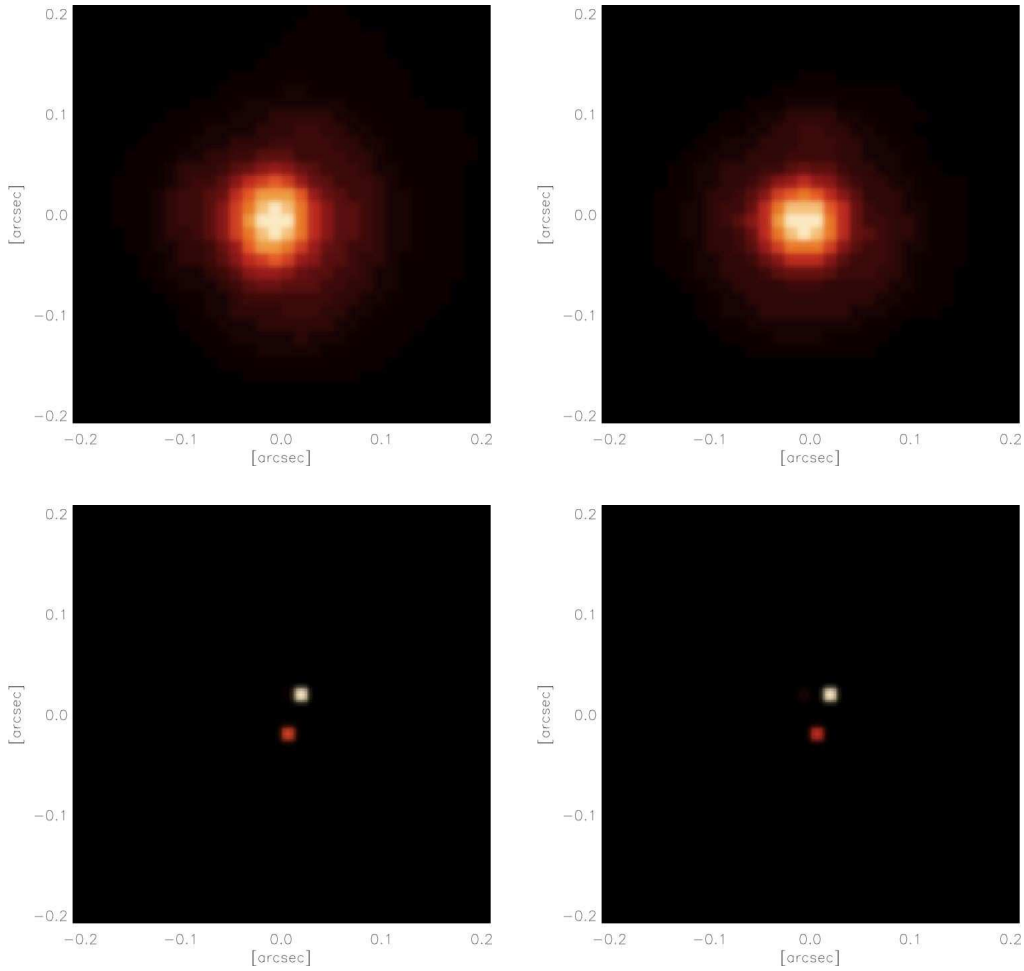

Fig. 1. From left to right and from top to bottom: post-NACO image of HD 87643, corresponding PSF, RL-based CSR reconstruction, RL-based SGP-accelerated CSR reconstruction. The resolution element is here $\lambda/D \simeq 56$ mas, corresponding to (a little bit more than) 4.3 px, the pixel size being of 13 mas. The binary separation found is $\rho \simeq 32$ mas $\simeq 2.45$ px $\simeq 0.57\,\lambda/D$.

The data pre-processing performed removed bad pixels, applied a flat-field correction, and also subtracted the sky background. Moreover, the PSF (estimated from images of the unresolved star HD 296986) was not exactly diffraction-limited since its FWHM was found to be 75 mas (see Millour et al. [14] for more details on these pre-processing points).

Figure 1 shows the results obtained by applying both our deconvolution-based CSR methods to our HD 87643 observations. A second set of data was also processed, giving fully similar results. Both results are also similar to the result obtained with the AMBER/VLTI data published in Millour et al. [14] Hence we can conclude that we have here fully validated our approach(es) of CSR.

HIP 113010 (HD 216405)

The data considered here are L'-band data (3.8-μm) obtained again with NACO/VLT. The resolution element is $\lambda/D \simeq 98$ mas, corresponding to (a little bit less than) 3.6 px, the pixel size being of $\simeq 27.2$ mas.

The observational conditions were good ones, leading to a Strehl ratio $\gtrsim 0.8$ in the observing waveband. Figure 2 shows the (pre-processed) image obtained. Component B (upper part of the image) was used as the PSF in order to deconvolve components AC (lower part of the image). In the same figure the results obtained with both methods employed are also shown and commented.

Although in this latter case the task is easier than previously because the binarity of the object could already be recognized in the pre-processed data (elongated shape clearly distinguishable from the PSF centro-symmetric shape), these results are also a matter for super-resolution.

Discussion

With the RL-based CSR algorithm 5000 iterations were performed for the first step and 1000 iterations for the second step. With in addition the SGP acceleration, the number of iterations were between $\sim$140 and $\sim$590 for the first step, and between $\sim$43 and $\sim$150 for the second step. The results are very similar in both cases.

Although the computational cost is heavier with SGP, we have at the end a resulting global speed-up between $\sim$7.5 and $\sim$24 when SGP is employed. In any case, and with such tiny regions of interest (in terms of number of pixels concerned by the object reconstruction process), computational times were in both cases quite small: between 14 s and 50 s for RL, and between 0.6 s and 6.7 s for SGP, on an Intel Core 2 Duo at 2.4 GHz. It is nevertheless worthwhile to note that, with a dedicated camera, with much more pixels per resolution element in order to fully take advantage from the CSR method, or simply by considering post-observational over-sampling of the data before applying our two CSR methods, this computational time gain would begin to be more interesting.

A last point concerns the photometric accuracy. No particular effort was made here, but our next-to-come step is to implement the third step of the procedure described in Anconelli et al. [6] and apply it to the data presented, permitting an a priori better reconstruction of the objects, and hopefully a quantitative comparison between the accuracies permitted with RL and SGP.

6 Summary and perspectives

In this paper we have presented a simple algorithm of CSR based on the very well known RL deconvolution method. An acceleration of it, based on the SGP method, is also presented in complement of the main one for possible acceleration of the reconstruction process. Both methods were tested and gave very encouraging results on two close binary stars observed with VLT/NACO in the wavebands K_s (for HD 87643) and L (for HIP 113010/HD 216405).

In the case of HD 87643, it has also been observed using the interferometric instrument AMBER onboard the VLTI and its binarity (half of the resolution limit of the VLT in band K_s) was clearly established with very similar results concerning the angular separation of the binary star, validating so our CSR approach in practice.

Further work on these data will concern first of all a careful pre-processing, with an estimation of the background to be used afterwards within the deconvolution method (rather than subtraction of it before deconvolution), then an over-sampling of the data before applying the CSR method(s), and, last but not least, an implementation of the third step of the

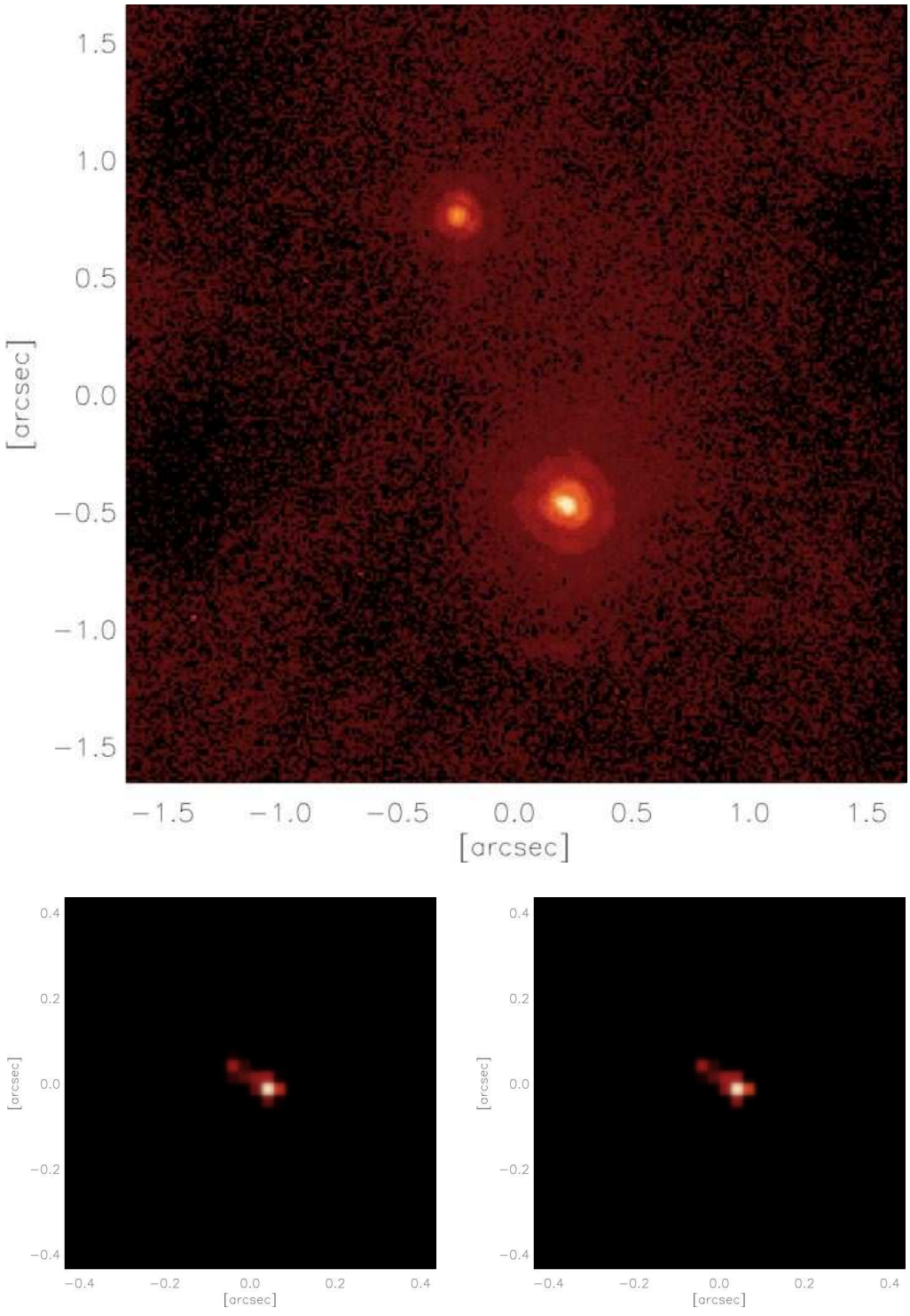

Fig. 2. From left to right and from top to bottom: post-NACO image of HIP 113010 (HD 216405), RL-based CSR reconstruction, RL-based SGP-accelerated CSR reconstruction. The binary separation found is $\rho \simeq 84\,\text{mas} \simeq 3.0\,\text{px} \simeq 0.86\,\lambda/D$.

method described in detail in Anconelli et al. [6] and permitting an a priori better reconstruction of the objects and hence a better quantitative comparison between the accelerated SGP method and the original RL one.

Finally note that this study has been performed by using the `Software Package AIRY` (see `http://airyproject.eu` for more details), developed within the `CAOS PSE` (see `http://lagrange.oca.eu/caos` for more details and to possibly freely download the last versions of both the `CAOS PSE` and the `Software Package AIRY`).

References

1. M. Bertero & P. Boccacci, *Micron* **34**, (2003) 265–273.
2. W. H. Richardson, J. Opt. Soc. Am. **62 (1)**, (1972) 55–59.
3. L. B. Lucy, Astron. J. **79**, (1974) 745–754.
4. M. Bertero & C. De Mol, *Progress in Optics XXXVI* (E. Wolf Ed., Elsevier, Amsterdam 1996) Chap. III.
5. M. Bertero & P. Boccacci, *Introduction to inverse problems in imaging* (IoP Publishing, Bristol 1998).
6. B. Anconelli, M. Bertero, P. Boccacci, M. Carbillet, Astron. Astrophys. **431**, (2005) 747–756.
7. S. Correia, M. Carbillet, P. Boccacci, M. Bertero, L. Fini, Astron. Astrophys. **387 (2)**, (2002) 733–743.
8. A. La Camera, M. Carbillet, C. Olivieri, P. Boccacci, M. Bertero, SPIE Proc. **8445**, (2012) 84453E–84453E-14.
9. M. Carbillet, C. Vérinaud, M. Guarracino, L. Fini, O. Lardière, B. Le Roux, A. T. Puglisi, B. Femenía, A. Riccardi, B. Anconelli, S. Correia, M. Bertero, P. Boccacci, SPIE Proc. **5490**, (2004) 550–559.
10. M. Carbillet, G. Desiderà, E. Augier, A. La Camera, A. Riccardi, A. Boccaletti, L. Jolissaint, D. Ab Kadir, SPIE Proc. **7736**, (2010) 773644–773644-8.
11. S. Bonettini, R. Zanella, L. Zanni, Inverse Prob. **25(1)**, (2009) 015002.
12. M. Prato, R. Cavicchioli, L. Zanni, P. Boccacci, M. Bertero, Astron. Astrophys. **539**, (2012) A133.
13. G. Rousset, F. Lacombe, P. Puget, N. N. Hubin, É. Gendron, T. Fusco, R. Arsenault, J. Charton, P. Feautrier, P. Gigan, P. Y. Kern, A.-M. Lagrange, P.-Y. Madec, D. Mouillet, D. Rabaud, P. Rabou, É. Stadler, G. Zins, SPIE Proc. **4839**, (2003) 140–149.
14. F. Millour, O. Chesneau, M. Borges Fernandes, A. Meilland, G. Mars, C. Benoist, É. Thiébaut, P. Stee, K.-H. Hofmann, F. Baron, J. Young, P. Bendjoya, A. Carciofi, A. Domiciano de Souza, T. Driebe, S. Jankov, P. Kervella, R. G. Petrov, S. Robbe-Dubois, F. Vakili, L. B. F. M. Waters, G. Weigelt, Astron. Astrophys. **507**, (2009) 317–326.
15. J.-B. Le Bouquin, F. Millour, A. Meilland, The Messenger **137**, (2009) 25–29.